GEOLOGICA
International Journal of Earth Sciences

VOLUME 9 NUMBER 1
ISSN 1025-2541
ISSN 3006-967X
WWW.GEOLOGICA.GOV.PK

GEOLOGICA

AN INTERNATIONAL JOURNAL OF EARTH SCIENCES

JULY
2024

BY
GEOSCIENCE ADVANCE RESEARCH LABORATORIES
GEOLOGICAL SURVEY OF PAKISTAN
WWW.GSP.GOV.PK

ISSN: 1025-2541
eISSN: 3006-967X

Siddiqui R.H., Ahmad M., Khan S., Azeem M., 2024. Geological Exploration and Genetic Modelling of Jol Khand Iron Ore, Baluchistan, Pakistan. Geologica v. 9, Article No. 1, Page 1-20.*
https://geologica.gov.pk/

GEOLOGICA
An International Journal of Earth Sciences

Geological Exploration and Genetic Modelling of Jol Khand Iron Ore, Baluchistan, Pakistan

[1]Rehanul Haq Siddiqui*, [2]Muqeet Ahmad [3]Sajjad Khan
[1]Saindak Metals Limited (SML), Quetta, Balochistan, Pakistan
[2]Pakistan Steel Mills, Karachi, Pakistan
[3]Geosciences Advance Research Laboratories, Geological Survey of Pakistan, Shahzad Town, 1461 Islamabad, Pakistan
*rehanhs1@gmail.com

Abstract

This study delves into the brief geological, mineralogical and geochemical aspects of iron deposits in the Jol Khand region of Balochistan, Pakistan. The Jol Khand iron ore deposit is situated within the Middle part of the Late Cretaceous Sinjrani Volcanic Group, constituting a significant component of the Chagai arc. The arc, extending approximately 500 km in length and 150 km in width with an east-west orientation, represents a vital geological feature in the western-north region of Pakistan, with extensions into Afghanistan and Iran. The deposit, characterized by lenticular bodies ranging from 35 cm to 5 m in thickness, is located in the Sinjrani Volcanics atop; a steep slope adjacent to the Jol Khand stream, approximately 27 km northeast of Chagai village. This study highlights the deposit's volcanogenic origin, emphasizing its superior quality and grade compared to other deposits within the Chagai arc. With an average iron content of 64.70 wt. % and an additional average of 1000 ppm of vanadium, the commercial potential of the ore is further enhanced. Initial estimates suggest iron ore resources in the area to be around 6.5 million tons. The ore is volcanogenic extrusive in origin, which was developed in the lower part of a subvolcanic upper-level magma chamber due liquid immiscibility of a Fe-rich homogenous silicate melt and subsequently erupted in a subaerial environment.

Keywords: Geological exploration, modelling, Jol Khand Iron ore, Pakistan

Introduction

Iron ore is a foundational element of modern industry, serving as the primary reservoir for extracting iron, a vital component essential for steel production and various alloys (Cloud, 1973; Galdon-Sanchez & Schmitz Jr., 2002). However, the significance of iron ores extends beyond industrial applications to encompass their diverse geological origins and formations worldwide. Iron deposits exhibit remarkable diversity in geological settings, ranging from deep-seated basic igneous intrusions to late-stage hydrothermal igneous, metamorphic, and sedimentary environments (Williams et al., 2005; Kazmi & Abbas, 2001). This diversity underscores the complex processes involved in the formation of these invaluable resources. In Pakistan, iron ore occurrences display notable diversity, encompassing various geological formations and compositions, from massive iron ores within igneous rocks of Nagarparkar to magmatic types in Balochistan and oolitic iron deposits in Khyber Pakhtunkhwa (Haider et al., 2018; Ahsan et al., 2008; Siddiqui et al., 1999; Chan, 1992). These deposits are distributed across diverse geological zones, illustrating the geological complexity of Pakistan's iron ore landscape (Kazmi & Abbas, 2001). Understanding the geological origins and formations of iron deposits is crucial for effective resource management and sustainable utilization of these invaluable assets. The present study relates to iron ore of Jol Khand area Baluchistan. Due to lack of detailed geochemical study done by previous workers in the area (Siddiqui, 1996; Siddiqui et al., 1986, 1987 & 1988; Ahmed (1984; Farah et al., 1984; Arthurton et al., 1979; Britzman, 1979; Dykstra, 1978; Nigell, 1975; Sillitoe, 1974; Vredenburg, 1901), this study focuses on providing a detailed examination of the mineralogical, geochemical, and genesis characteristics, along with assessing the economic viability of the Jol Khand Region in Balochistan.

Geotectonic Setting

The Jol Khand iron ore deposit emerges as one of the latest additions to the volcanogenic ore reserves within the Chagai arc, situated approximately 27 km northeast of Chagai village (Fig. 1). Geographically, the area is delineated by latitudes 29º 27' 15.19" N - 29º 27' 47.15" N and longitudes 64º 30' 36.69" E - 64º 31' 03.14" E, as depicted on Topographic Sheet No. 34C/11, positioned at the northeastern edge of a small plateau adjacent to Malik Ali Koh, known as the Jol Khand plateau. Accessing this deposit presents a considerable challenge, as the plateau is encircled by steep cliffs from all directions (Fig. 1), with no jeep-able roads available. Presently, reaching the deposit necessitates a challenging climb of approximately one and a half hours from the southeastern side of the plateau. Geologically, the Jol Khand deposit is situated within the Middle part of the Late Cretaceous Sinjrani volcanic Group (Figs. 1 and 2; Siddiqui., 1996; Bakr & Jackson., 1964). This deposit is located in the north-central segment of the Chagai belt, also referred to as the Chagai arc, Chagai hills, or Chagai anticlinorium, positioned within the Balochistan province of Pakistan. This region hosts a multitude of significant metal deposits, including porphyry (Cu-Mo-Au-), manto and vein type copper, stratiform and skarn type iron, volcanogenic gold-silver and sulphur, as well as kuroko type lead-zinc-silver-copper, intimately associated with the magmatic rocks of the arc. Additionally, various granites and green onyx marble (travertine) have been reported within this arc. The Chagai-Makran region represents a distinctive tectonic setting within the eastern Middle East, bounded by the Makran subduction zone to the south, characterized as one of the few surviving subduction zones of Cretaceous age. Notably, other subduction zones in the region, such as the Indus suture zone in the Himalayas and Zagros subduction in Iran, have been obliterated by major continental collisions. The Makran region is further demarcated by the Chaman transform fault to the east and the Harirud fault to the west. Much of the southern Makran region comprises one of the largest accretionary prisms globally, situated on the hanging wall of the Makran subduction zone. This accretionary prism extends for 450 km to the north, where it converges against two mountain ranges, Chagai and Raskoh, representing the magmatic arc of the Makran subduction zone. The Chagai magmatic arc extends north into Afghanistan, exhibiting Cretaceous to Quaternary magmatism akin to the Chagai arc (Shareq et al., 1977).

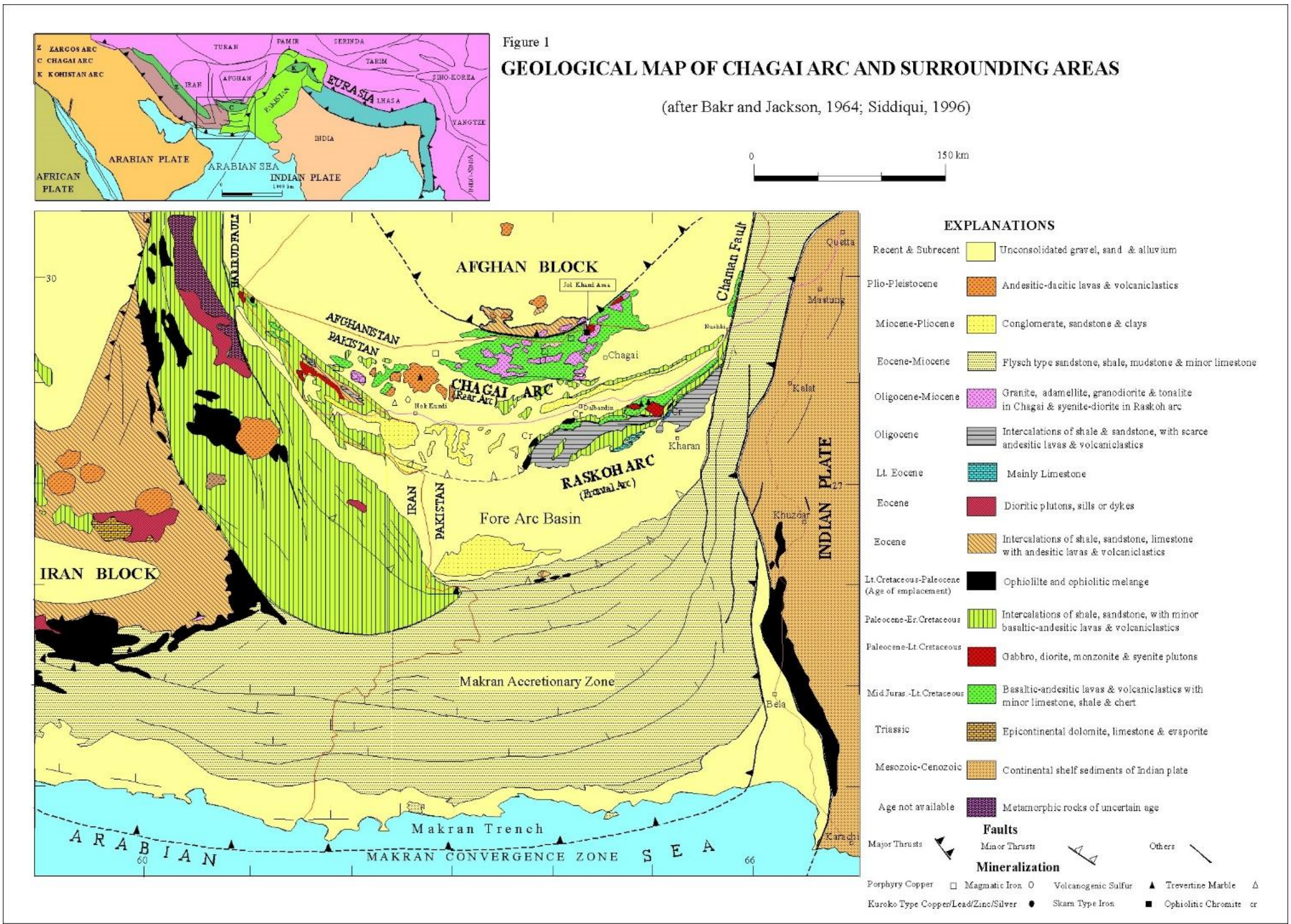

Fig. 1 Geological Map of Chagai and surrounding area showing the location of the study area (Modified after Bakr and Jackson., 1964; Siddiqui., 1996).

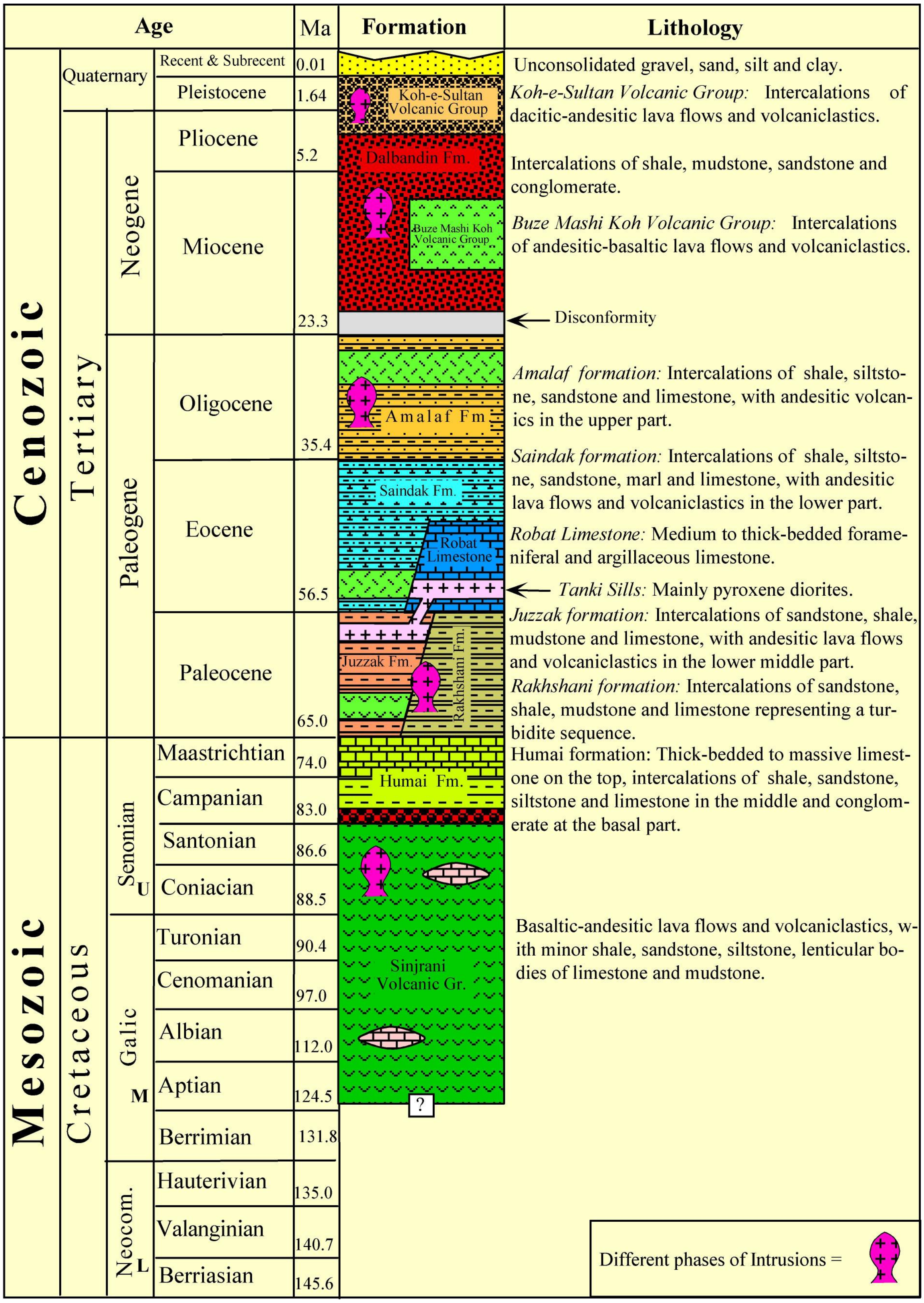

Fig. 2a Generalized stratigraphic sequence in Chagai arc (Modified after Siddiqui, 1996; Jones, 1960). The ages in the time scale are after Cohen et al., 2022.

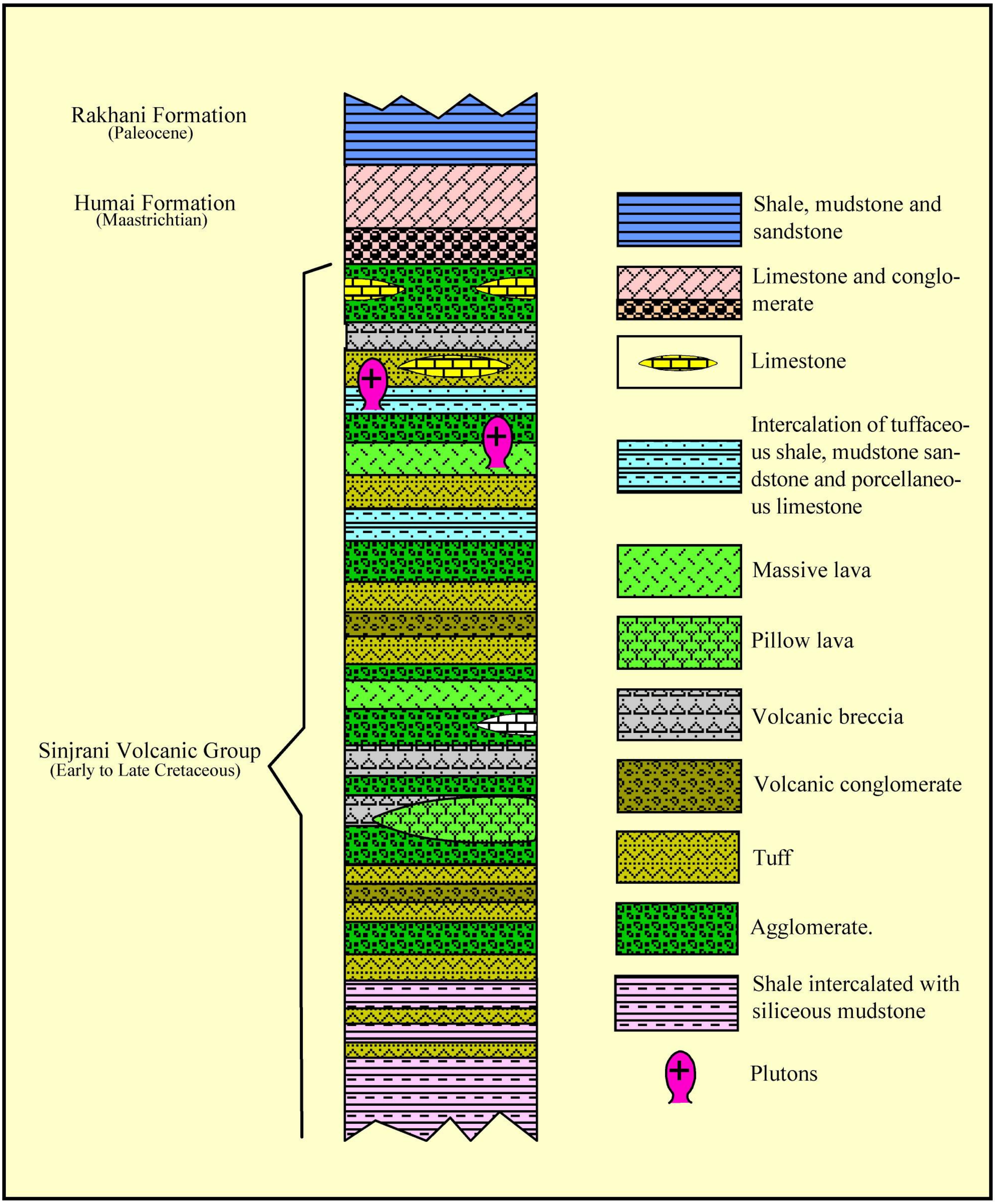

Fig. 2b Detailed internal stratigraphy of Sinjrani volcanic Group (Siddiqui et al., 2017).

Methods

The investigation focused on iron deposit of area involving measurements, and sampling for finding mineralogical, geochemical, and genesis identification, along with assessing the economic viability. After reconnaissance and selection of the area a detailed field was decided for sampling and field data collection. Besides geological mapping, the sections were measured and almost seven samples were collected randomly from the section. The formation is sampled from bottom to top. Special care was taken to maintain sample integrity by storing them in sample bags to prevent contamination. Field samples along with detailed observations of the outcrop were also conducted to assess field-related information. Elemental analysis of major and trace elements was conducted at the Geoscience Laboratory, Geological Survey of Pakistan, Islamabad, utilizing X-ray fluorescence spectrometry (RIGAKU XRF-3370E). Sample powders (< 200 mesh) were meticulously blended with lithium tetra borate (flux) in a 1:10 sample to flux ratio. The resulting glass beads were then subjected to XRF analysis. Table 1 showcases the values obtained from 05 samples extracted from the Jol Khan iron ore (Table 1), alongside analytical data from renowned iron ore deposits in Pakistan and globally (Table 1 & 2).

Results

Field Observations

The field study revealed that the oldest rock formation in the Jol Khand area is the Late Cretaceous Sinjrani Volcanic Group (Fig. 3a-d), characterized by undifferentiated basaltic to andesitic lava flows and volcaniclastics, including agglomerate, volcanic conglomerate, breccia, and tuff. Additionally, there are subordinate amounts of tuffaceous mudstone, claystone, and siltstone, particularly in the middle part of the Group (Fig. 4a-g & 5a-g). These rocks exhibit a northeast to east-west striking orientation with dips ranging from 10 to 20 degrees towards the southeast. The flows appear dark green to black, weathering to a brownish-black hue. They typically display porphyritic characteristics with phenocrysts of pyroxene and plagioclase. Basaltic-andesites and andesites are prevalent rock types in the area. Weathering has resulted in extensive propylitic alteration, evidenced by the presence of chlorite, epidote, and calcite. Certain tuffaceous mudstones and siltstones exhibit abundant iron concretions (Fig. 4a-g & 5a-g). In the northern and part of the Jol Khand plateau, the Sinjrani Volcanic Group rocks are intruded by sections of a large batholith of adamellites and a small diorite stock belonging to Chagai Intrusions (Fig. 3). Adamellite appears light pinkish grey when fresh and weathers to light greyish brown. It primarily comprises plagioclase, orthoclase, quartz, mica, and minor hornblende. Diorite, on the other hand, is greenish grey when fresh, weathering to greyish brown, and is mainly composed of partially to completely chloritized hornblende and partially argillized plagioclase. The area is also intersected by two left-lateral strike-slip faults in the middle part of the mapped area (Fig. 3). Subsurface geology in the area is delineated in geological cross-sections along lines AB (Fig. 3b), CD (Fig. 3C), and EF (Fig. 3d).

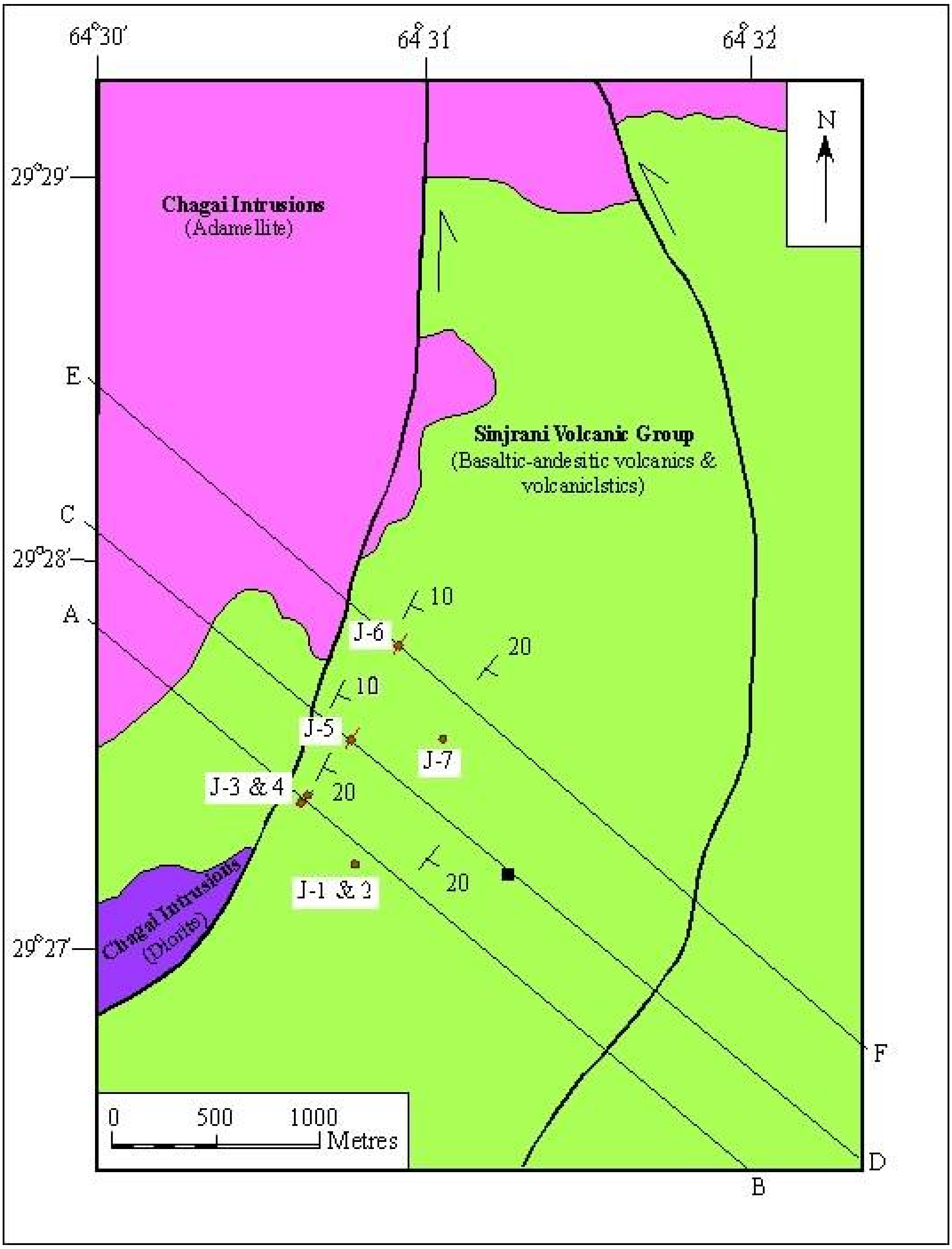
64°30′
64°31′
64°32′
29°29′
29°28′
29°27′
N
Chagai Intrusions
(Adamellite)
Sinjrani Volcanic Group
(Basaltic-andesitic volcanics & volcaniclstics)
Chagai Intrusions
(Diorite)
E
C
A
F
D
B
J-6
J-5
J-7
J-3 & 4
J-1 & 2
10
20
0
500
1000
Metres

(a)

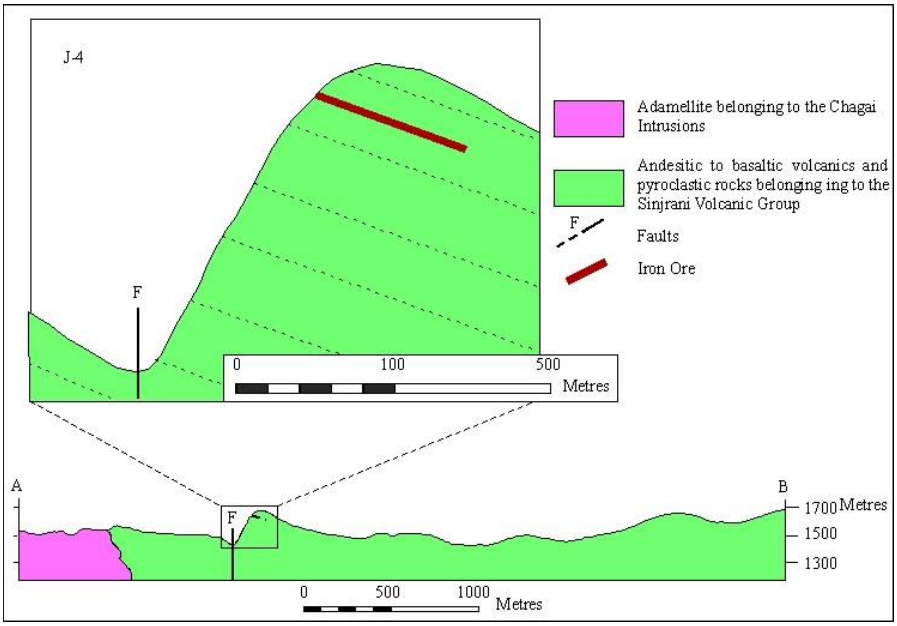
J-4
Adamellite belonging to the Chagai Intrusions
Andesitic to basaltic volcanics and pyroclastic rocks belonging ing to the Sinjrani Volcanic Group
Faults
Iron Ore
F
0 100 500 Metres
A
B
1700 Metres
1500
1300
0 500 1000 Metres

(b)

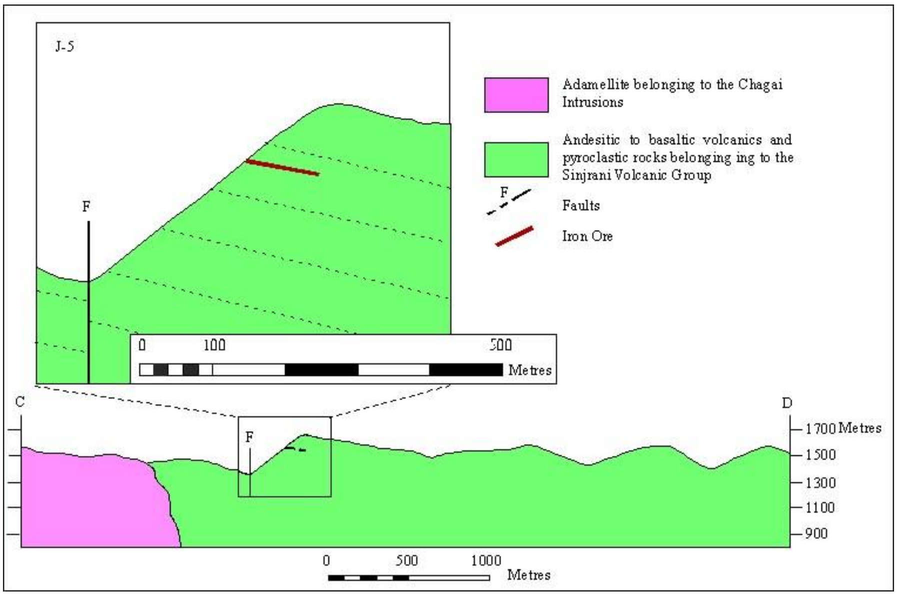
J-5
Adamellite belonging to the Chagai Intrusions
Andesitic to basaltic volcanics and pyroclastic rocks belonging ing to the Sinjrani Volcanic Group
Faults
Iron Ore
F
0 100 500 Metres
C
D
1700 Metres
1500
1300
1100
900
0 500 1000 Metres

(c)

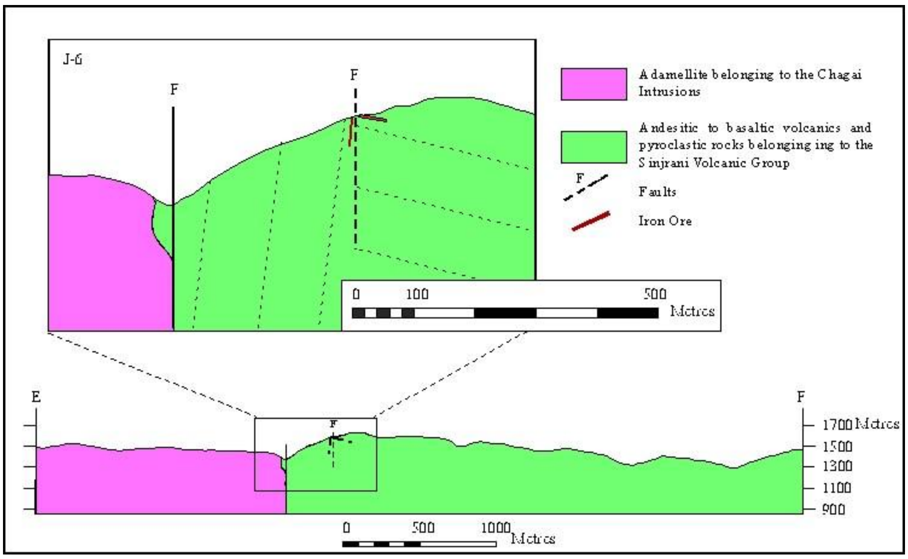
J-6
Adamellite belonging to the Chagai Intrusions
Andesitic to basaltic volcanics and pyroclastic rocks belonging ing to the Sinjrani Volcanic Group
Faults
Iron Ore
F
0 100 500 Metres
E
F
1700 Metres
1500
1300
1100
900
0 500 1000 Metres

(d)

Fig. 3 Comprehensive geological explanation of the study area; (a) Detailed geological Map of Jol Khand area, (b) Geological cross section along the line AB, (c) Geological cross section along the line CD, and (d) Geological cross section along the line EF.

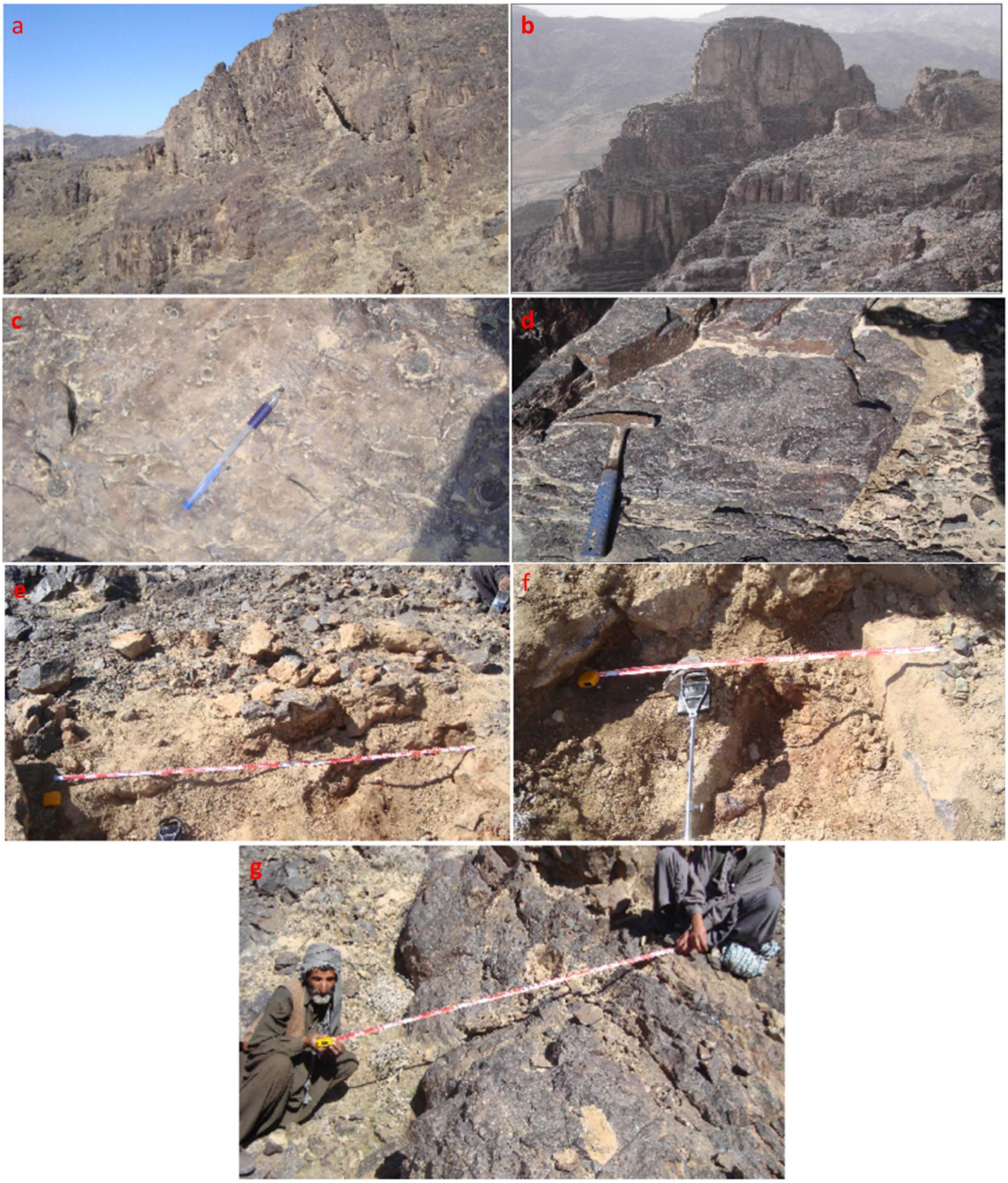

Fig. 4 Field photos exhibiting field descriptions; (a) A gently dipping volcanic and volcanoclastic rocks belonging to the Late Cretaceous Sinjrani Volcanic Group in Jol Khand area, (b) Different cycles of eruption in the volcanic rocks belong to the Late Cretaceous Sinjrani Volcanic Group in Jol Khand area, (c) Iron well rounded stone concretion within the tuffaceous mudstone belonging to the Late Cretaceous Sinjrani Volcanic Group in Jol Khand area, (d) Iron concretion within the tuffaceous mudstone belonging to the Late Cretaceous Sinjrani Volcanic Group in Jol Khand area, (e) A partially exposed martite body at J-1, (f) A partially exposed martite body at J-2, and (g) A 2 m thick composite body of martite and epidotized andesite at J-3. This composite body strike in NNE direction and dips 5E.


a
b
c
d
e
f
g

Fig. 5 Field photos demonstrating field descriptions; (a) A 80 cm thick body of martite near J-3, (b) A view of 5m thick composite body of martite and epidotised andesite. This composite body strikes in NE direction and dips 20E and occurs at J-4, (c) Part of a 3m thick body of a martite near J-4, (d) View of 4m thick martite body at J-5, (e) A view of 5m thick martite body at J-5, (f) A view of 2m thick martite body at J-6, which strikes N20E and dips 85W and (f) Another view of 2m thick martite body at J-6, which strikes N20E and dips 85W.

Geochemistry

The XRF analysis unveiled that the concentration of iron (Fe) in the Jol Khand ore deposit (samples J-2 to J-6) varies between 60.74 and 67.04 wt.%, with an average of approximately 64.70 wt.% (Table 1). Additionally, the ore exhibits lower levels of phosphorus (P) ranging from 0.00 to 0.02 wt.%, titanium (Ti) ranging from 0.006 to 0.40 wt.%, and sulfur (S) ranging from 0.01 to 0.18 wt.%. The vanadium content in the Jol Khand iron ore deposit spans from 0.00 (observed in only one sample) to 3412 ppm, with an average concentration of around 1000 ppm.

Table 1 Bulk chemical composition of the Jhol Kand iron ore, along with a comparative analysis against several renowned iron deposits within the Chagai arc. All measurements are expressed in weight percent (%), except for vanadium values, which are denoted in parts per million (ppm).

Oxides	J-2	J-3	J-4	J-5	J-6	Average Chigandik	Average Pachinkoh	Average Chilghazi
SiO2	5.16	8.76	3.47	4.19	3.05	19.95	15.60	11.72
TiO2	0.04	0.02	0.08	0.01	0.02	-	-	-
Al2O3	0.41	0.38	0.54	0.18	0.31	2.71	4.41	0.30
Fe2O3	90.79	86.84	94.25	94.82	95.84	-	-	-
MnO	0.20	0.42	0.14	0.16	0.11	-	-	-
MgO	0.19	0.52	0.10	0.10	0.16	-	-	-
CaO	0.87	1.98	0.54	0.26	0.33	-	-	-
Na2O	1.87	0.22	0.00	0.23	0.22	-	-	-
K2O	0.00	0.00	0.02	0.00	0.00	-	-	-
P2O5	0.00	0.03	0.017	0.00	0.00	-	-	-
Ti	0.024	0.012	0.40	0.006	0.00	-	-	-
Fe	63.50	60.74	65.92	66.32	67.04	43.60	50.00	51.87
P	0.00	0.013	0.007	0.00	0.00	0.10	0.10	0.10
S	0.013	0.178	0.036	0.025	0.013	1.71		0.10
V	980	290	3412	0.00	381	-	-	-

Table 2 Range and average concentration of major Jhol Kand iron ore and its comparison with some of the famous iron ore deposits of the world. The value in column 1 is after Siddique et al., 2024. 2 is after Siddiqui et al., 1999; in columns 3 to 5 are from Jensen and Bateman, 1981 and values in column 6 to 9 are from Ohle, 1972. All the values are in wt %.

Oxides	Jol Khand Average	Nizampur Average	Dilband Average	Clinton USA	Superior Canada	Minette Europe	Itabira Brazil	Tofo Chile	Kiruna Swede n	Mesabi USA
		1	2	3	4	5	6	7	8	9
SiO_2	4.926	34.16	19.45	11.42	48.35	28.06	8.40	0.80	1.97	3.18
TiO_2	0.034	1.11	0.33	0.015	0.01	0.18	0.008	0.150	0.067	0.351
Al_2O_3	0.364	15.24	6.58	5.07	0.48	5.79	0.84	1.80	0.50	11.48
Fe_2O_3	92.508	41.50	50.72	74.051	48.57	44.34	82.98	90.13	94.92	90.42
MnO	0.206	0.02	0.03	0.17	0.025	0.16	1.68	0.10	7.04	7.080
MgO	0.214	0.24	1.88	0.63	0.32	1.54	0.00	traces	0.00	0.21
CaO	0.796	0.29	7.04	3.32	0.1	1.92	0.17	traces	0.01	0.72
Na_2O+ K_2O	0.5174	0.32	0.17	ND	0.34	0.86	-	-	-	-
P_2O_5	0.0094	0.14	1.01	1.961	0.039	1.589	0.133	0.115	1.112	0.271
Fe	64.704	28.82	35.45	51.76	33.95	30.99	58.00	63.00	66.35	63.20
P	0.004	0.06	0.44	0.855	0.017	0.693	0.058	0.05	0.485	0.118
S	0.053	0.03	1.0	0.023	0.013	ND	0.012	0.020	0.008	0.073
V	1012.6	0.058	0.068	-	-	-	0.00	0.00	0.00	0.010

Economic Potential

In the study area iron ore mineralization is spread in a 1.25 km x 300 m area, which trends in a NE-SW direction. The mineralization occurs in the middle part of the Sinjrani Volcanic Group (Figs. 3a-d, 4a-g and 5a-g). Iron ore is represented mainly by martite (a mixture of magnetite and hematite). The mineralization occurs in the cliff forming upper part of the southeastern bank of a small stream, locally known as Jol Khand. The martite occurs as lenticular bodies: range in thickness from 35 cm to 5 metres and extends up to 150 metres (due to extremely difficult approach and time-constraint full extent of all the bodies were not observed, therefore had to depended on the statements of keen local observers). These lenticular bodies occur in the andesitic rocks belonging to the middle part of the Sinjrani Volcanic Group and generally follow the local trend of these rocks. The iron mineralization is observed in four localities including J-1 to J-7. In J-1 (Fig. 4e-f) and J-7 localities ore is not fully exposed and of poor quality, whereas at J-3 to J-6 locations, ore is of good to excellent quality (Fig. 3). At J-3 (N 29° 27' 22.4", E 64° 30' 37.74" two martite bodies each 35 cm thick are separated by a 1.3 m thick bed of epidotized andesite. This body strike in the NNE direction and dips 5° - 10° E. These two bodies merge to a 80 cm body of martite (Figs. 4g and 5a). At J-4 (N 29° 27' 20.70", E 64° 30' 37.02") two bodies of 1.5 at margins and one body of one metre thick is intercalated with epidotized andesite. These bodies strike in NNE direction and dip 20° E and merges to form a 3 m thick martite body (Fig. 5b-c) at (N 29° 27' 21", E 64° 30' 37.05"). At J-5 (N 29° 27' 31.2", E 64° 30' 52.2") a 4 m thick vertical body of martite is exposed which strikes in N 10○ E. Very near to J-5 at (N 29° 27' 31.68", E 64°

30’ 52.32”) a 5 m thick body of martite is found (Fig. 5d-e), which strikes in E-W direction and dips 10° SE, which indicates the existence of a fault between the two bodies. At J-6 (N 29° 27’ 47.04”, E 64° 31’ 1.62”) a 2 m thick body of martite is well exposed, which strikes in N 20° E and dips 85° W (Fig. 5f-g). The total exposed length of this body is 14 m. A few metres towards east, across a fault another body of martite is found which is 2.5 m thick, which strikes in N 20° E and dips 10° W. The length of this body is 16 m. Subsurface extension of these bodies are represented in geological cross sections along the lines AB (Fig. 3b) CD (Fig. 3c) and EF (Fig. 3d). At J-2 (N 29° 27’ 11.76”, E 64° 31’ 36.72”) a partially exposed lenticular body of martite is found within the gently dipping volcanic rocks. Another body of martite is partially exposed at J-7 (N 29° 27’ 31.62”, E 64° 31’ 5.82”).

Ore Grade and Tonnage

The iron concentration in the Jol Khand ore deposit (J-2 to J-6) ranges 60.74 to 67.04 wt. % and averages about 64.70 wt. % (Table 1). The ore has lower P (0.00 to 0.02 wt %), Ti (0.006 to 0.40 wt %) and S (0.01 to 0.18) range, which enables the ore most suitable for processing and beneficiation in the steel industry. The vanadium concentration in the Jol Khand iron ore deposit ranges from 0.00 (only in one sample) to 3412 ppm and averages about 1000 ppm. The higher contents of V in the ore have further enhanced its commercial values. The V can be obtained as by product from the iron ore. The initial reserve estimation and evaluation studies indicate about 6.5 million ton of iron ore resources in the area. However exact ore reserves in the area may be calculated after detailed magnetic and gravity surveys and exploratory drilling etc.

Discussions

Iron ore deposits exhibit diverse geological origins, encompassing sedimentary, magmatic, and hydrothermal environments (Gutzmer et al., 2009; Fard et al., 2017; Haruna et al., 2017; Nakhaeiand Irannajad, 2018; Salawu and Saliu, 2021). Predominantly, around 90% of the world's iron ore deposits originate from Precambrian sources, notably banded iron ore deposits formed through chemical precipitation in early oceanic waters (Klein and Beukes, 1992; Klein and Ladeira, 2000; Trendall, 2002). Conversely, approximately 10% of iron ore deposits stem from magmatic and metasomatic skarn-type origins (Broughm et al., 2017; Ovalle et al., 2018; Salazar etal., 2020; Sarjoughian et al., 2020). Various processes contribute to the genesis of these deposits, including diagenetic, syngenetic, and deep-seated hydrothermal mechanisms (Sales, 1962;

Ridge, 1976; Sillitoe et al., 2017). Magnetite-type iron ores, often associated with dense-phase magmatism, undergo active gravitational settling in magma chambers, leading to layering and cumulate formations (Edmonds et al, 2015a; Edmonds, 2015b; Zallmer and Edmonds, 2015; Ovalle et al., 2018; Edmonds and Wood, 2018). The geochemistry of magnetite provides crucial nsights into deposit sources and ore-forming processes, with crystallization occurring within andesitic magma chambers under specific conditions (Wang et al., 2017). Additionally, globally recognized iron deposits, such as those near El Laco in Chile (Park, 1961; Frutos and Oyarzun, 1975; Henriquez and Martin, 1978) and Cerro de Mercado in Mexico (Ramirez-Lara, 1973; Van Allen, 1978; James and Lyons, 1988), attest to the significance of extrusive processes in iron ore formation.

The fine-grained texture with sparse vesiculations, stratiform-lenticular occurrence and intercalations with stratified basaltic to andesitic volcanic and volcanoclastic rocks suggest a volcanogenic extrusive origin of the Jol Khand iron ore (Figs. 3a-d, 4a-g and 5a-g). Higher concentration of vanadium and lower abundances of titanium and sulphur in the ore further confirm its magmatic origin. As stated earlier that basaltic to andesitic volcanic and volcaniclastic suites in which Jol Khand iron ore found; belong to tholeiitic assemblage of Late Cretaceous Sinjrani Volcanic Group(Siddiqui et al., 2017). The parent magma of this assemblage had been interpreted to have generated by 15–20% partial melting of a depleted sub-arc mantle source and fractionated in an upper-level magma chamber (Siddiqui et al., 2017). It is farther suggested that ferric oxide silicate magma was developed due to high oxygen fugacity resulted due to the heavy influx of volatiles from the subducting plate into the sub-arc mantle magma source (Fig. 6). It is insinuated that the liquid magnetitic magma fraction was separated from a homogeneous iron enriched silicate magma due to liquid immiscibility in a upper-level subvolcanic magma chamber. The denser iron oxide (magnetite) magma was accumulated in the lower part of the magma chamber and subaerially erupted through an adjacent fault conduit (Fig, 6). Martitization was developed just after the eruption of magnetite lava when it was still hot.

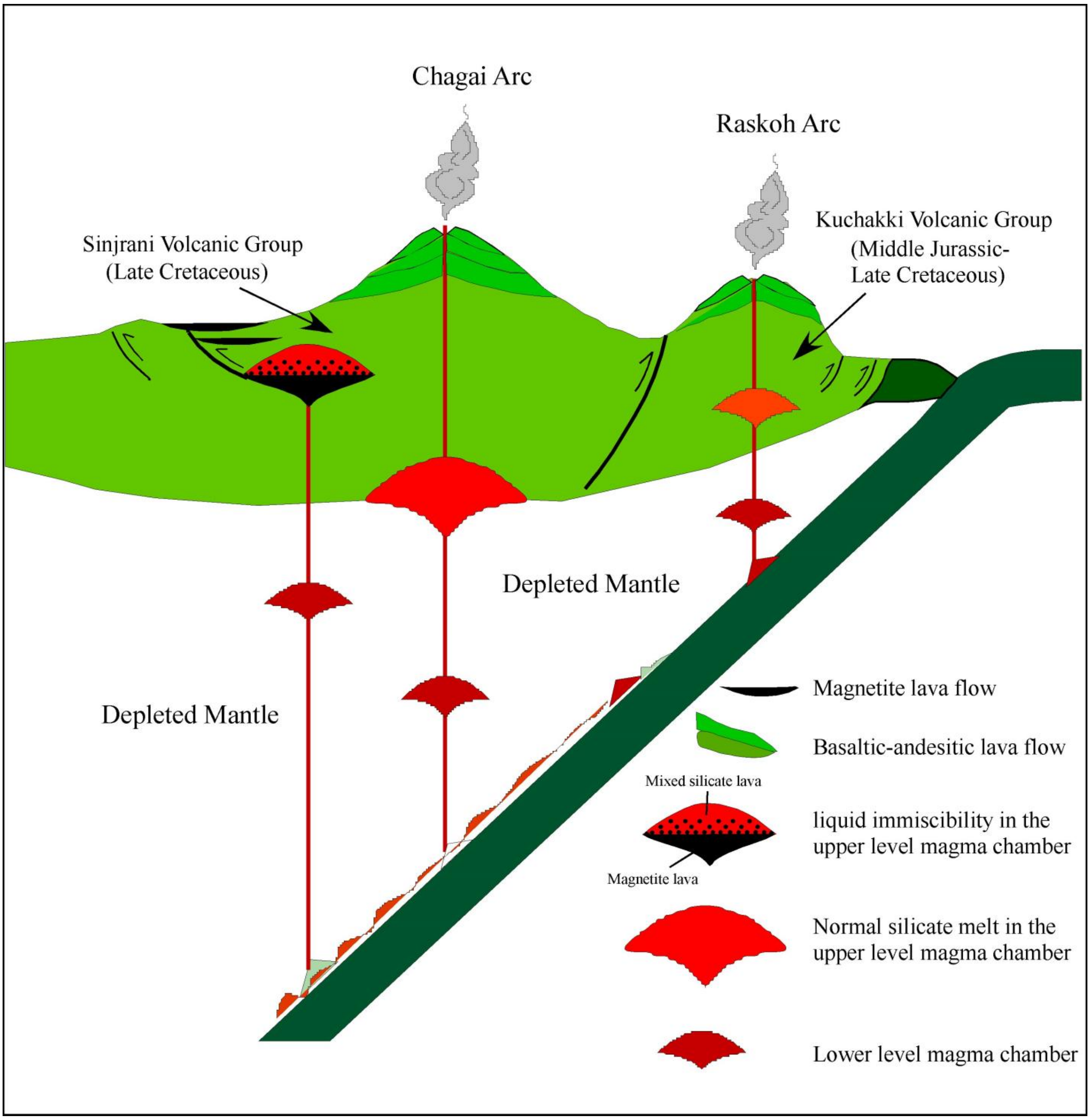

Fig. 6 Model illustrating the liquid immiscibility in an upper magma chamber and eruption of magnetitic lava flow in Jol Khand area, Chagai arc.

Conclusions

The comprehensive field investigations and initial laboratory studies conducted in the Jol Khand area has provided valuable insights into its economic potential and initial genetic modelling. The studies indicate that the Jol Khand iron ore with an average iron content of 64.70 wt. % is one of the best iron ore so far discovered in the Chagai arc. The higher average contents of vanadium (1000 ppm) in the ore further enhance its commercial value. The ore is developed in the middle part of a basaltic-andesitic volcanic and volcaniclastic sequence of Late Cretaceous Sinjrani Volcanic Group. The ore (magnetite) is volcanogenic extrusive in nature, which was developed in lower part of a subvolcanic upper-level magma chamber due liquid immiscibility of a Fe-rich homogenous silicate melt and subsequently erupted in a subaerial environment through fault conduit. The magnetite ore is martitized just after its subaerial eruption. Detailed mineralogical and geochemical studies are recommended for final genetic modelling.

Magnetic/gravity surveys and drilling at various locations of are recommended for further accurate reserve calculations.

Acknowledgements

The authors extend their heartfelt appreciation to the officers and staff of M/S Pacific Mining and Explorations Pvt., Ltd. for their outstanding coordination of accommodations and logistical support at the base camp in Jol Khand. Furthermore, Mr. Shabir Ahmad is acknowledged for his assistance in arranging boarding and lodging accommodations in Dalbandine. Special gratitude is also extended to GARL, Geological Survey of Pakistan, Islamabad, for their invaluable laboratory analysis services.

References

Ahmed, M. U., 1984. Geological exploration and preliminary evaluation of Dasht-e-Kain porphyry copper-molybdenum prospect Chagai district, Balochistan, Pakistan. Unpublished Ph.D. thesis Univ. Belgrade, Yugoslavia.

Ahsan, S N., Firdous, R., Mastoi, A S., Ghuryani, S. (2008). Dhedro iron oxide-gold+ copper prospect a preliminary evaluation, Nagar Parker, Tharparker district, Sindh Pakistan. . Publication Directorate GSP Quetta,872, 1-40.

Arthurton, R. S., Alam, G. S., Ahmed, S. A. and Iqbal, S., 1979. Geological history of Alam Reg -Mashki Chah area, Chagai District, Balochistan. In Farah, A. and DeJong, K. A., (eds.), Geodynamics of Pakistan. Geol. Surv. Pakistan, 325-331.

Bakr, M. A. and Jackson, R. O., 1964. Geological Map of Pakistan. Geol. Surv. Pakistan, Quetta.

Britzman, L., 1979. Fission track ages of intrusives of Chagai District, Balochistan, Pakistan. Unpubl. M.A. thesis, Darmouth College, Honover, N. H., U.S.A.

Broughm, S. G., Hanchar, J. M., Tornos, F., Westhues, A., Attersley, S. (2017). Mineral chemistry of magnetite from magnetite-apatite mineralization and their host rocks: examples from Kiruna, Sweden, and El Laco, Chile. Mineralium Deposita, 52 (8), 1223-1244

Cloud, P. (1973). Paleoecological significance of the banded iron-formation. Economic Geology, 68(7), 1135-1143.

Chan, M A. (1992). Oolitic ironstone of the Cretaceous Western Interior seaway, east-central Utah. Journal of Sedimentary Research, 62(4).

Dykstra, J. D., 1978. A geological study of Chagai Hills Balochistan, Pakistan using LANDSAT digital data. Ph.D. Thesis (unpublished), Dartmouth College, Hanover, N. H., U.S.A.

Edmonds, M., Woods, A. W. (2018). Exsolved volatiles in magma reservoirs. Journal of Volcanology and Geothermal Research, 368, 13-30.

Edmonds, M., Brett, A., Herd, R. A., Humphreys, M.C. S., Woods, A. (2015 b). Magnetite-bubble aggregates at mixing interfaces in andesite magma bodies. Geological Society, London, Special Publications, 410 (1), 95-121.

Frutos, J. J., and Oyarzun, J. M., 1975, Tectonic and geochemical evidence once rningth e genesiso f El Lacom agnetitela vaf low deposits Chile: ECON.G EOL.,v . 70, p. 988-990.

Henriquez,F ., and Martin,R . F., 1978, Crystal-growth textures in magnetite flows and feeder dykes, E1 Laco, Chile: Canadian Mineralogist, v. 16, p. 581-589.

Galdon-Sanchez, J. E., Schmitz Jr, J. A. (2002). Competitive pressure and labor productivity: world iron-ore markets in the 1980's. American Economic Review, 92 (4), 1222-1235.

Gutzmer, J., Beukes, N. J., De Vivo, B., Grasemann,B., Stüwe, K. (2009). Iron and manganese oredeposits: mineralogy, geochemistry, and economic geology. Encyclopedia of Life Support Systems. UNESCO, Paris, 43-69.

Haider, N., Khan, S., Rashid, M.U., Siddiqui, R.U., Zeb, J., Iqbal, S., Khan, A., Ahmad, W., 2018. Geochemistry and Petrographical Study of Langrial Iron Ore from Tethyan Hazara Area Pakistan, with Emphasis on its Economic Characterization and Depositional Setting. Int. J. Econ. Environ. Geol., 9 (2), 40-48.

Haruna, A. I., Umar, U. S., Mohammed, A. A., Maude,K. A (2017). Geochemistry and Economic Potential of Jaruwa Iron Ores, NW-Nigeria. Imperial Journal of Interdisciplinary Research, volume (3), 1067-1074.

Jones, A. G., 1960.. Reconnaissance Geology of Part of West Pakistan. A Colombo Plan Cooperative Project, Govt. of Canada, Toronto, (Hunting Survey Corporation report) 550.

Kazmi, A., Abbas, S. (2001). Metallogeny and mineral deposits of Pakistan. Islamabad, Pakistan, Orient Petroleum.

Klein, C., Beukes, N. J. (1992). Proterozoic iron-formations. In: Developments in Precambrian Geology, Elsevier, 10, 383-418.

Klein, C., Ladeira, E. A. (2000). Geochemistry andpetrology of some Proterozoic banded iron-formations of the Quadrilátero Ferrífero, MinasGerais, Brazil. Economic Geology, 95 (2), 405-427.

Nakhaei, F., Irannajad, M. (2018). Reagents types inflotation of iron oxide minerals: A review.Mineral Processing and Extractive Metallurgy Review, 39 (2), 89-124.

Nigell, R. H., 1975. Reconnaissance of the geology and ore mineralization in part of the Chagai District, Balochistan, Pakistan. Project Report PK-27, U. S. Geol. Surv., 550.

Shareq, A., Chmyriov, V. M., Stazhilo-Alekseev, K. F., Dronov, V. I., Gannon, P. J., Lubemov, B. K., Kafarskiy, A. K. H. and Malyarove, E. P., 1977. Mineral Resources of Afghanistan. (2nd ed.), Afghan Geol. and Mines Surv., Afghanistan.

Ovalle, J. T., La Cruz, N. L., Reich, M., Barra, F.,Simon, A. C., Konecke, B. A. Morata, D. (2018).Formation of massive iron deposits linked toexplosive volcanic eruptions. Scientific reports, 8(1), 1-11.

Park, C. F., Jr., 1961, A magnetite "flow" in northern Chile: ECON. GEOL., v. 56, p. 431-441.

Ramirez~Lara, M. A., 1973, Unidad La Perla: Asoc. Ingenieros
Minas, Metalurgistas Geologos Mexico, Conveneion Nat., X,
Chihuahua, Mem., p. 27-46.

Ridge, J. D. (1976). Origin, development, and changesin concepts of syngenetic ore deposits as seen by North American Geologists1. In Classificationsand Historical Studies (pp. 183-297). Elsevier.

Salazar, E., Barra, F., Reich, M., Simon, A., Leisen,M., Palma, G. Rojo, M. (2020). Trace element geochemistry of magnetite from the Cerro NegroNorte iron oxide−apatite deposit, northern Chile. Mineralium Deposita, 55 (3), 409-428.

Sarjoughian, F., Habibi, I., Lentz, D. R., Azizi, H., & Esna-Ashari, A. (2020). Magnetite compositions from the Baba Ali iron deposit in the Sanandaj-Sirjan zone, western Iran: Implications for oregenesis. Ore Geology Reviews, 126, 103728.

Sales, R. H. (1962). Hydrothermal versus syngenetic theories of ore deposition. Economic Geology, 57(5), 721-734.

Sillitoe, R. H., Perelló, J., Creaser, R. A., Wilton, J.,Wilson, A. J., Dawborn, T. (2017). Age of the Zambian Copper belt. Mineralium Deposita, 52(8), 1245-1268.

Salawu, S. I., & Saliu, A. M. (2021). Characterization and beneficiation of Obajana iron ore, Kogi State,Nigeria. Acta Technica Conveniences-Bulletin of Engineering, 14 (4), 105-108.

Siddiqui, R. H. Jan, M. Q., Khan, M. A., Kakar M. I., Foden, J. D. 2017, Petrogenesis of the Late Cretaceous Tholeiitic Volcanism and Oceanic Island Arc Affinity of the Chagai Arc, Western Pakistan. Acta

Geologica Sinica (English Edition). 91 No. 4, 1248–1263)

Siddiqui, R. H., Hussain, S. A. and Haque, M., 1987. Geology and petrography of Eocene mafic lavas of Chagai island arc, Balochistan, Pakistan. Acta Mineralolgica Pakistanica, 3, 123-128.

Siddiqui, R. H., Haque, M. and Hussain, S. A., 1988. Geology and petrography of Paleocene mafic lavas of Chagai island arc, Balochistan, Pakistan. Geol. Surv. Pakistan, I. R. No. 361, 18.

Siddiqui, R. H., Khan, W. and Haque. M., 1986. Petrololgical and petrochemical studies of northcentral Chagai Belt and its tectonic implications. Acta Mineralogica Pakistanica, 2, 12-23.

Siddiqui, R. H., 1996. Magmatic evolution of Chagai-Raskoh arc terrane and its implication for porphyry copper mineralization. Geologica, 2, 87-119.

Siddiqui, R. H., Mengal, J. M., Haider, N. (1999). First occurrence of late magmatic iron associated with ophiolite complex in Khanozai area Balochistan, Pakistan. GEOLOGICA, 4(1), 123-134.

Siddiqui, R. H., 2004. Crustal evolution of the Chagai-Raskoh arc terrane, Balochistan, Pakistan. Unpublished PhD Thesis, Centre of Excellence in Geology, University of Peshawar, Pakistan.

Sillitoe, R. H., 1974. Metallogenic evolution of a collisional mountain belt in Pakistan. Geol. Surv. Pakistan, Rec., 34, 16.

Vredenburg, E. W., 1901. A geological sketch of the Balochistan desert and part of Eastern Persia. Geol. Surv. India, Mem., 302.

Trendall, A. F. (2002). The significance of iron-formation in the Precambrian stratigraphic record. Precambrian sedimentary environments: A modern approach to ancient depositional systems,33-66.

Val Allen, B., 1978, Hydrothermal iron ore and related alterations in the volcanic rocks of La Perla, Chihuahua, Mexico: Unpub. M.A. thesis, Austin, Univ. Texas, 131 p.

Wang, F., Bagas, L., Jiang, S., Liu, Y. (2017). Geological, geochemical, and geochronological characteristics of Weilasituo Sn-polymetalic deposit, Inner Mongolia, China. Ore Geology Reviews, 80, 1206-1229.

Williams, P. J., Barton, M. D., Johnson, D. A., Fontboté, L., De Haller, A., Mark, G., Oliver, N H., Marschik, R. (2005). Iron oxide copper-gold deposits: Geology, space-time distribution and possible modes of origin. Economic Geology, 371-405

Manuscript received 17 March 2024;
Revision accepted May 13 2024;
Published 25 July 2024

"COLLABORATE WITH GEOLOGICA, EMBRACE THE FUTURE OF EARTH SCIENCES"

CONTACT US

Email Address:

info@geologica.gov.pk

Website Address:

www.geologica.gov.pk

Phone Number:

+92-51-9255135

Office Address:

Geoscience Advance Research Laboratories,
Geological Survey of Pakistan,
Park Road, Link Kuri Road, Shehzad Town,
Islamabad

JULY
2024

GEOLOGICA

AN INTERNATIONAL JOURNAL OF EARTH SCIENCES

CONTACT US
+92-51-9255135
INFO@GEOLOGICA.GOV.PK
WWW.GEOLOGICA.GOV.PK